Effect of the Glass-Transition Temperature on Film Formation in 2-Ethylhexyl Acrylate/Methyl Methacrylate Emulsion Copolymers

Linda A. Cannon and Richard A. Pethrick*

Department of Pure and Applied Chemistry, Thomas Graham Building, University of Strathclyde, 295 Cathedral Street, Glasgow G1 1XL, Scotland

Received February 24, 1999; Revised Manuscript Received June 28, 1999

ABSTRACT: The effect of the glass-transition temperature [T_g] of the latex on the film-formation behavior of a series of 2-ethylhexyl acrylate/methyl methacrylate emulsion copolymers is reported. Stage 1 of film formation was studied using a combination of dynamic mechanical analysis and conductivity measurements. Stages 2 and 3 were investigated using calorimetric compensation, differential scanning calorimetry, dielectric spectroscopy, and atomic force microscopy. Comparison of the results from the different methods employed leads to a detailed model of the film-formation process in which the temperature used relative to the minimum film-formation temperature determines the effectiveness of the processes. The relative usefulness of the techniques used in their ability to characterize the various stages in the film-formation process is discussed for these copolymers systems.

Introduction

The problem of defining the various stages involved in film formation in acrylic latex systems has been discussed recently.[1−5] A wide range of techniques have been applied to the study of this process.[1−9] This paper focuses on characterization of the channel structure generated within the film as the particles agglomerate to form a homogeneous film. Data are presented in this paper using some methods that have hitherto not been used widely for the investigation of film formation. It is generally agreed that evaporation is the dominant rate-limiting process in film formation when the temperature of a latex is about 20 K or more above its glass-transition [T_g] temperature. When a latex is nearer to its T_g, the rate-limiting step in film formation is deformation of the particles, driven by the desire to reduce the surface energy. The initial stages of film formation are associated with loss of solvent, leading to a touch dry film that will still contain significant quantities of moisture. Subsequent drying leads to collapse of the voided structure initially formed to create a densely packed structure. The nature of the drying fronts which develop in the film has been the subject of detailed consideration.[5−9] The drying front tends to attempt to achieve vertical homogeneity, and the packing process is driven by capillary pressure. Whether the particles undergo coalescence to form a completely homogeneous film will depend on a number of factors of which the T_g is one. There is evidence that a drying front first creates microvoids in the loosely packed film structure. Evaporation rates are retarded in a latex that is well above its T_g, probably as a result of the reduced surface area of water caused by extensive particle deformation. Sperry and co-workers[10] have suggested that there are two important stages in the process of latex film formation: evaporation of the aqueous solvent and deformation/compaction of particles leading to void closure. They postulate that either of these steps could be rate-limiting, depending on the temperature of the process.

A study of the nature of the aqueous filled channels as a function of time using dielectric analysis can provide new insight into this critical stage of the film-formation process and is the subject of this paper. Copolymers of 2-ethylhexyl acrylate (EHA)/methyl methacrylate (MMA) having film-formation temperatures[11] that range from below to above room temperature have been selected for this study. These materials have previously been studied using multiple angle of incidence ellipsometry and environmental SEM[11] and a range of other methods. These techniques detect the transition from a liquid dispersion to a film through changes in the optical clarity or particle density. Although many latex films attain optical clarity fairly rapidly, full coalescence can, however, take several days.

This paper attempts to probe these longer time processes using dielectric analysis and a range of related methods selected to probe specific aspects of the film-formation process. The study falls into two parts: investigation of the pseudoliquid phase (stage 1) and the second part considers the processes occurring in the touch dry films.

Experimental Section

Materials. The monomers used were obtained from Aldrich and were purified before use. Vinyl monomers are inhibited with hydroquinone or hydroquinone monomethyl ether, which can be removed by washing with NaOH solution saturated with NaCl.[12]

Synthesis and Characterization of the Latex Polymers. The polymerization was carried out in a 1 L reaction flask fitted with a lid, a condenser, a nitrogen line, a thermometer, and two dropping funnels. The same scheme was used in all of the latex preparations, and a stirring rate of 200−250 rpm was maintained throughout the process. The aqueous charge was added to the reaction vessel and purged with nitrogen for 30 min to remove oxygen and then heated to 50 °C with a nitrogen blanket covering the mixture. The redox initiator seed was added in three parts, with a 10 min equilibration time between each addition. Subsequently, the monomer seed was added, and the charge was stirred vigorously for 10 min. The color of the emulsion gains a blue tinged white color, and the temperature rises by about 7 °C. The initiator and monomer feeds are added over a period of 3 h, with careful monitoring of the temperature and stirring rates.

* To whom communications should be addressed.

10.1021/ma990273i CCC: $18.00
Published on Web 10/15/1999

Table 1. 2-Ethylhexyl Acrylate/Methyl Methacrylate Copolymers Latexes Prepared

latex	composition MMA/EHA%	% nonvolatiles	MFFT (K)	mean particle size (nm)	T_g DSC (K)	M_w/M_n
CoME1	74.8:25.2	29.9	>333	97.7	355	857 00/219 000
CoME2	54.3:45.8	30.8	322	92.0	327	1 715 000/222 000
CoME3	48.8:51.3	28.6	319	97.4	317	1 290 000/172 000
CoME4	43.9:56.1	31.5	300	97.7	304	1 091 000/137 000
CoME5	30.9:69.1	40.1	288	113.7	286	977 00/98 150

After addition of the feed, a mop-up shot was added (this addition of further redox initiator quenches any free monomer in the latex), and the mixture was left to react for 30 min. The compositions of the latex copolymers prepared are summarized in Table 1.

Standard Formulation for Emulsion Polymerization of coMEX. The aqueous charge consisted of 57 g of water, 0.06 g of sodium dodecyl sulfate (SDS), and 0.23 g of disodium hydrogen phosphate (DHP). The procedure used involved the stagewise addition of initiator: seed 1, 0.004 g of potassium persulfate (KPS) (aq); seed 2, 0.045 g of sodium metabisulfite (SMBS) (aq); seed 3, 0.004 g of KPS (aq). The formulations are derived from a recipe by Sommer et al.[13]

Latex Characterization. A small amount of each latex was dried and analyzed by FTIR. The dried latex sample was dissolved in chloroform and spotted onto a sodium chloride disk. The FTIR spectra of the five latex copolymers all exhibit the characteristic bands associated with acrylates; these are as follows: 2995 cm^{-1}, C−H $str_{(asymmetric)}$; 2953 cm^{-1}, C−H $str_{(symmetric)}$; 1730 cm^{-1}, C═O str; 1271, 1240 cm^{-1}, C−O−$C_{(asymmetric)}$; 1190, 1148 cm^{-1}, C−O−$C_{(symmetric)}$; 1027 cm^{-1}, C−C−O ester; and 989, 842 cm^{-1}, ester skeletal vibration. There was no evidence for residual monomer in the polymer. Elemental analysis of the five dry polymers was also obtained; this was carried out by the microanalysis and was in agreement with the formula in Table 1.

General Methods of Characterization of the Latex Materials. *Minimum Film-Formation Temperature (MFFT).* A stainless steel bar heated at one end with thermocouples distributed along its length provides a controlled temperature gradient. A glass plate covered the bar and was allowed to equilibrate for 2 h with nitrogen passed along its length to ensure a constant humidity. A Mayer bar was used to achieve a constant film thickness of latex dispersion deposited on the heated surface. After the latex had dried, the MFFT was defined as the point where a clear film was observed to have formed, Table 1.

Glass-Transition Temperature (T_g). The T_g's of the dried films were determined by differential scanning calorimetry (DSC) with a Perkin−Elmer DSC-2 using temperature scans from 243 to 403 K at 10 °C s^{-1}, at a sensitivity range of 5 mcal s^{-1}, Table 1.

Solids Content of the Emulsions. The percentage of nonvolatiles−solid content (% nv) was determined from the initial and final weights after drying at 80 °C overnight; % nv = (final weight)/(initial weight) × 100. To minimize the error in this measurement, the samples were cooled to room temperature before reweighing, Table 1.

Particle Size Determination. The mean particle size was measured using a Malvern Autosizer 2C, which has a range from 0.003 to 3 μm, Table 1.

Molecular Weight Determination. The analysis of the copolymer latexes was performed by RAPRA Technology, Ltd., using gel permeation chromatography (GPC) and dimethylformamide (DMF) as the solvent. A Plgel 2 X mixed bed-B, 30 cm, with 10 μm columns, was used with ammonium acetate-buffered DMF as eluent and a flow rate of 1.0 mL/min. Poly(methyl methacrylate) (PMMA) standards were used to calibrated the GPC, and all the results are quoted as "PMMA-equivalent" molecular masses.

First Stage of Film Formation. The transformation of emulsion in to a solid film was followed using two techniques.

Dynamic Mechanical Analysis. A Rheovibron-DDV II C was adapted to monitor the change in mechanical properties of a substrate coated with the latex as the solution dries. A suitable substrate, No. 1 Whatmann filter paper, 9 × 45 mm^2 was held between two clamps, with one connected to a stress transducer and the other to a strain gauge. A force, P, is applied to a strip of material of length, l, and cross-sectional area, A, and the stretched length is Δl. The longitudinal stress is P/A, and the longitudinal strain is $\Delta l/L$. Young's modulus of the solid, E, is defined as follows:

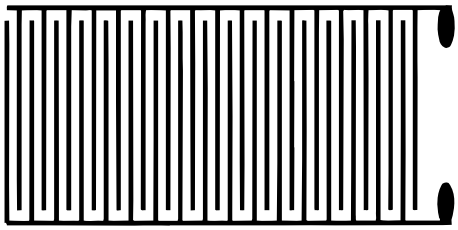

Figure 1. Schematic of electrode used in conductivity measurements.

$$\frac{\text{stress}}{\text{strain}} = \frac{P/A}{\Delta l/l} = \frac{Pl}{A\Delta l} = E \qquad (1)$$

The strain transducer output is a voltage that was fed to a computer. The stress applied by the rheovibron is fixed, and the measured strain will depend on the modulus of the sample. A 50 μL sample of emulsion was applied to the substrate using a micropipet, and the analysis continued until a constant voltage reading was obtained. Because the paper has the possibility of a small variability in its modulus, the traces are quoted in terms of the change in voltage (strain) with time rather than attempting to calculated the absolute modulus values. Profiles were obtained at different drying temperatures and drying rates determined from the slope of the voltage versus time curve. Values of the rate were measured over a range of temperatures and were used to generate an Arrhenius plot:

$$\ln(\text{rate}) = \frac{-E_a}{R}\frac{1}{T} + C \qquad (2)$$

where E_a is the activation energy, R is the gas constant, T is the temperature, and C is a constant reflecting the mechanism of the process for the film formation.

Conductance Measurements. Conductance was measured using a 1286 Electrochemical Interface connected to a BBC computer. The electrodes, Figure 1, were made from positive-resist-coated double-sided copper-clad board (RS Components) using photolithography. A volume of 1 mL of latex was applied to the electrode using a Mayer bar draw-down apparatus, producing a film of latex of thickness 0.1 mm. The change in the conductivity as the film dried was measured. The measuring voltage was 0.01 V, the resistance of the electrodes was 100 Ω, and the time interval between analyses was 30 s.

Stages 2 and 3 of Film Formation: Maturation of the Latex Films. When the latex film is macroscopically (touch) dry, other techniques can be applied to the study of the films.

Calorimetric Compensation Method.[14,15] The measurements were performed using the Perkin−Elmer DSC-2 using temperature scans from 243 to 403 K at 10 °C s^{-1}, at a sensitivity range of 5 mcal s^{-1}, which can discriminate between reversible and irreversible processes occurring in a latex film. The samples were cast into a flat Petri dish and dried for 24 h.

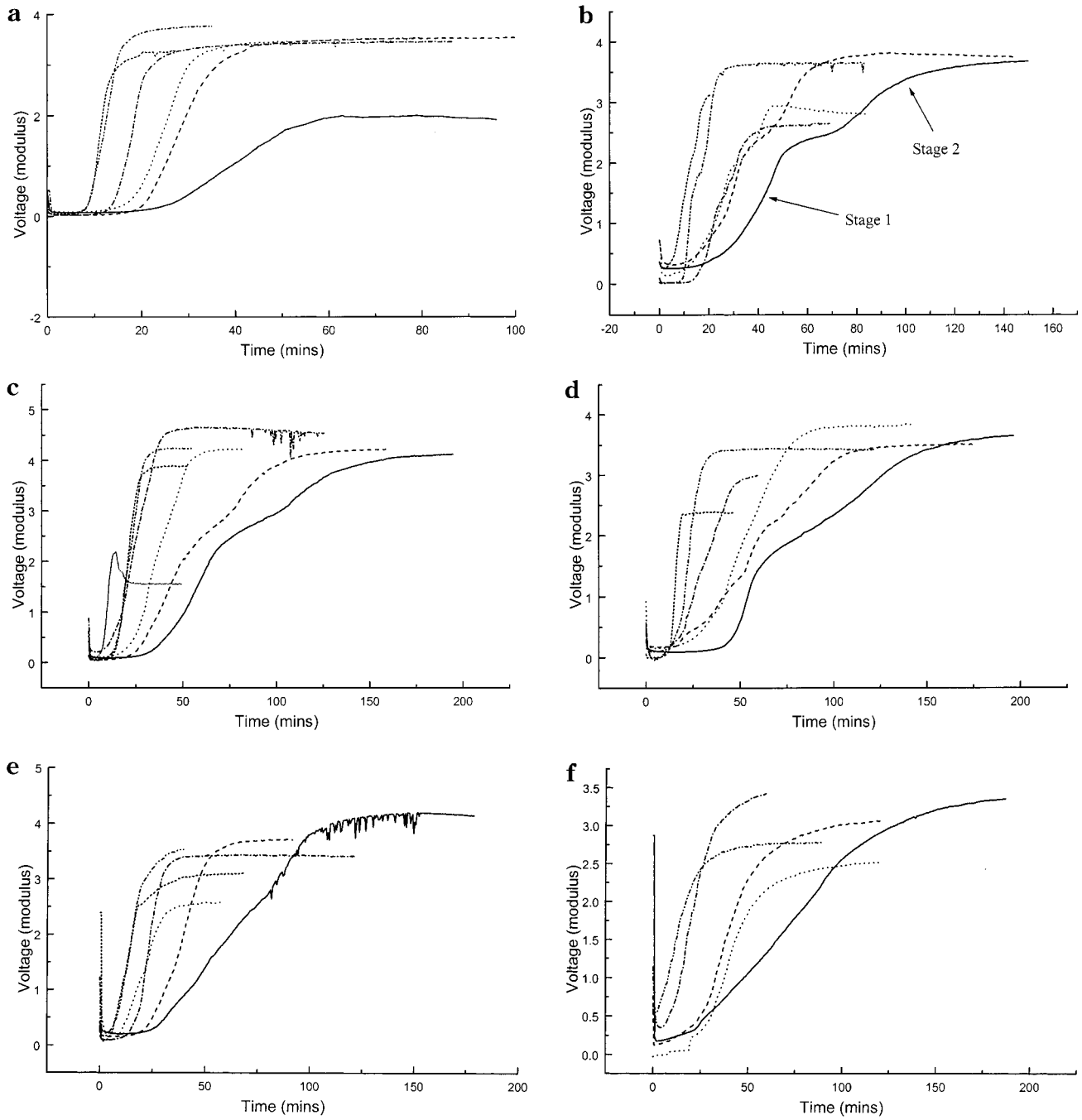

Figure 2. Dynamic mechanical profiles obtained using a filter paper substrate for drying with the following: (a) water, (b) coME1, (c) coME2, (d) coME3, (e) coME4, and (f) coME5. Key: ─ 295 K, ─ ─ ─ 304 K, --- 307 K, ─•─ 313 K, ─••─ 323 K, and ··· 323 K.

Two samples identical in weight to within 2%, were placed in two sample pans of identical weight, to within 0.1 mg. The analysis was performed in three consecutive steps:• Step 1: A dried latex sample was placed in the sample holder, and a temperature scan was performed against an empty reference pan. The scan was terminated before the latex-decomposition temperature.

• Step 2: After the calorimeter is cooled to ambient temperature, the sample was carefully transferred to the reference holder. A fresh sample was placed in the sample holder, and the thermal scan was repeated. The sample in the reference holder will display the reversible thermal changes, whereas the fresh sample in the sample holder will show both reversible and irreversible changes. Two types of irreversible change can occur: one, disappearance of the surface of the latex and, two, coalescence and destruction of crystalline regions in the film. These latex films are amorphous.

• Step 3: After the sample was cooled, a second run was performed to generate a baseline.

This method allows for the identification and separation of reversible and irreversible thermal changes. The method can be applied to the measurement of the enthalpy of coalescence of latex films and the identification of crystalline domains.

Dielectric Spectroscopy. Measurements were performed using a technique that has been described previously.[16] Analysis of the dielectric properties was performed over the range 10^{-1} to 6×10^5 Hz and over a temperature range from 270 to 355 K. The latex sample was coated with silver-loaded epoxy, which was used as the electrode for the study. The method used for analysis of latex films has been described previously.[12]

Atomic Force Microscopy (AFM). A Burleigh AFM was used in the study of the changes in surface structure with aging time. Latex samples were cast onto a section of silicon wafer and allowed to dry; they were subsequently scanned at regular

intervals during maturation. The software can perform several forms of statistical analyses on the image data. Values of R_q, defined in terms of the root-mean-square variation of the height along a line defined in the surface can be expressed as the following:

$$R_q = \sqrt{\frac{1}{N}\sum_i^N (Z_i - Z_{avg})^2} \quad (3)$$

and R_a is the height variance of the line/surface, given by

$$R_a = \frac{1}{N}\sum_i^N |Z_i - Z_{avg}| \quad (4)$$

and R_{p-p} is the height difference between the highest and lowest points on the line/surface, given by

$$R_{p-p} = Z_{max} - Z_{min} \quad (5)$$

As the value of Z_i tends toward Z_{avg} the statistical quantity decreases, indicating a decrease in the surface roughness of the sample.[17]

Results, Analysis, and Discussion

Characterization of the Latex Copolymers Used in the Study. The latexes contain varying ratios of MMA and EHA, and the composition variation influences the physical nature of the resultant film. MMA is a high T_g polymer (378 K) and EHA is a low T_g polymer (188 K); therefore a reduction of the percentage of MMA present in the copolymer decreases the T_g of the latex film. The basic physical properties of these latexes have been measured, Table 1. The mean particle size and particle size distributions are essentially the same for the five copolymers.

First Stage of Film Formation. *Dynamic Mechanical Analysis.* The five latex samples and a reference study using water were analyzed using a Rheovibron−DDV IIC. The film formation occurs on a paper substrate and leads to an enhancement in the modulus as the film is formed. The drying profile of pure water was initially determined at the same temperatures as those subsequently used for the study of the latex samples, Figure 2a. The rate of drying was determined from the initial slope of the drying profiles and was measured as a function of temperature. The temperature dependence of the drying rates were then used to determine the activation energy for the drying processes. Evaporation of water, Figure 2a, shows a simple profile; however, coME1, Figure 2b, shows a more complicated drying profile. The gradient of the drying curve changes several times during the drying process and is indicative of a multistage process. Increases in the drying temperature cause the profile to simplify to a single-stage process. Differences in the way in which the drying processes takes place as the temperature is varied can be associated with the ability of the particles to undergo deformation, reflected in the T_g values of the copolymers. The drying profiles of the lower T_g latexes, Figure 2d,e, exhibit a single-stage profile. The drying profiles can be classified on the basis of two different models, Figure 3.

A Single-Stage Drying Model. The process described in this model, Figure 3a, can be divided into four stages. (a) Plasticization of the substrate by the latex solution.

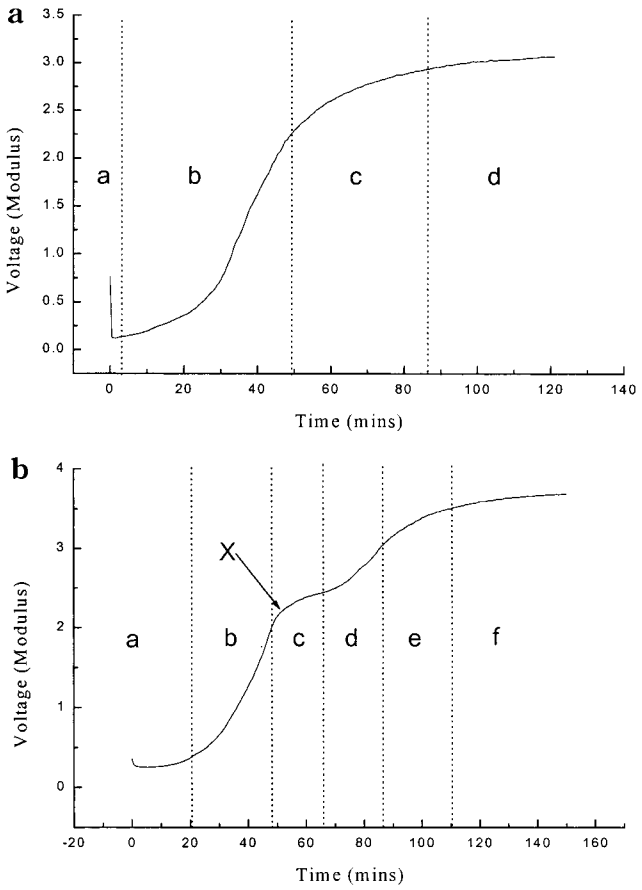

Figure 3. Drying model: (a) single- and (b) two-stage process.

The latex is absorb into the paper substrate, which softens it, resulting in a reduction in the observed modulus. (b) Evaporation of water. During this stage of the process, an increase in the modulus is observed associated with film formation of the latex. Water evaporation leads to the substrate modulus increasing, and the close packing of the latex particles resulting in film formation enhances this effect. (c) Reduction of the rate of evaporation. The majority of water has been lost from the system, and the evaporation kinetics slow and eventually stop. (d) Constancy of the modulus region, where nearly all of the water has been lost. The time period for the expulsion of residual water is dependent on the latex itself and can be days or weeks.

A Two-Stage Model. The two-stage model, Figure 3b, involves a more complex scheme in which six stages can be identified. (a) Plasticization of the sample substrate. (b) Evaporation of water and buildup in mechanical strength. (c) Falling of the rate period, observed in this region at a much earlier stage than in the previous model. The evaporation kinetics are slowed by the requirement to deform the particles to achieve film formation. (d) Evaporation of the water, leading to an increase in the T_g of the film and an increase in the modules. (e) and (f) Slow coalescence of particles and the occurrence of film formation.

Stage c in model 2 is of great importance as it splits drying into a two-stage model at point X. Point X occurs when the modulus is 0.7(final modulus). Assuming that evaporation kinetics follow a first-order mechanism, then point X occurs at a 0.7 volume fraction of solids in the forming polymer film. The usually accepted volume filling fraction for spherical particles corresponds to 0.76. This type of profile is seen only in high T_g polymers

Table 2. Temperature for a Single-Stage Drying Process in Relation to MFFT

description	stage 1 E_a (drying rate) (kJ mol^{-1})	stage 2 E_a (drying rate) (kJ mol^{-1})	MFFT (K)	single-stage process temp. (K)
water	40.3 ± 2.4			
co-ME1	43.3 ± 4.2	47.5 ± 2.1	>333	>323
co-ME2	41.3 ± 5.2	70.9 ± 4.1	322	322
co-ME3	55.6 ± 3.5		319	>313, <323
CoME4	43.8 ± 5.3		300	>294, <304
CoME5	45.5 ± 3.9		288	<293

dried at low temperatures. The drying rate was used to generate Arrhenius plots and calculate activation energies for the drying process, Table 2.

The activation energy calculated for evaporation of water correlates well with the literature value for the enthalpy of evaporation, 40.3 kJ mol^{-1}. The calculated stage 1 activation energies for all of the copolymers are close to that of the enthalpy of evaporation of water, implying that water evaporation is the dominant process. A two-stage drying profile is observed for coME1 and coME2 and in the lower temperature regions of coME3. The emergence of the second stage occurs at approximately 0.7 volume fraction and is associated with the effects of deformation influencing the drying rate.[14−17] Comparison of the rate constants and activation energies for stage 1 in coME1 and coME2 with those of water drying, indicates that for low T_g polymers the rate approximates that of the water evaporation process.

Stage 2 of the drying process in coME1 and coME2 has a higher activation energy. A similar tendency is observed in the data for coME3−5, Figure 2d−f. These latexes display a single-stage water evaporation-controlled drying profile.

The emergence of stage 2 at a 0.7 volume fraction is explained in terms of the influence of the T_g of the polymer. During film formation, water evaporates at a constant rate until the particles form a densely packed structure.[18] The evaporation rate then decreases and deformation of the particles occurs so that they fill all of the available space. High T_g latexes will have a higher resistance to deformation; therefore, more energy will be required to promote the final stages of film formation in these systems, resulting in the characteristic two-stage drying profile of latexes dried below their film-formation temperature. As the T_g of these latexes decreases, the particles will deform more readily and the rate of increase in the mechanical strength increases as shown in Figure 2b−e. In addition, as the temperature of the drying environment tends toward the MFFT of the latex, the magnitude of stage 2 diminishes and the increasing dominance of stage 1 becomes evident. This effect is exemplified for coME4 and coME5, where the low T_g of these MFFT latexes exhibit only a single-stage drying profile.

Table 2 summarizes the temperature at which the latex exhibited a single-stage drying profile and its MFFT. Above its MFFT, the latex will dry in a single stage, indicating that the polymer particles resistance to deformation is diminishing and that evaporation is the dominant process. The temperature at which the drying process shifts from a two-stage to a single-stage mechanism can be identified as the minimum film-formation temperature of the latex.

Keddie et al.[11] have identified that for films dried below their MFFT there exists a transitional drying

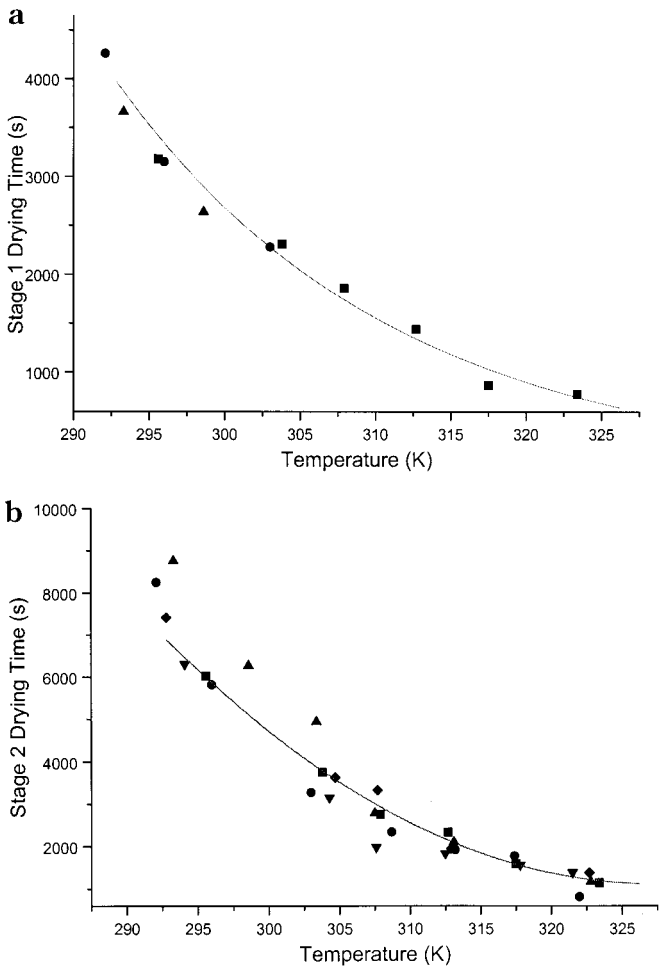

Figure 4. Plot of (a) stage 1 drying time vs temperature and (b) stage 2 drying time vs temperature. Key: ─ coMEK E1, ● coMEK E2, ▲ coMEK E3, ▼ coMEK E4, and ◆ coMEK E5.

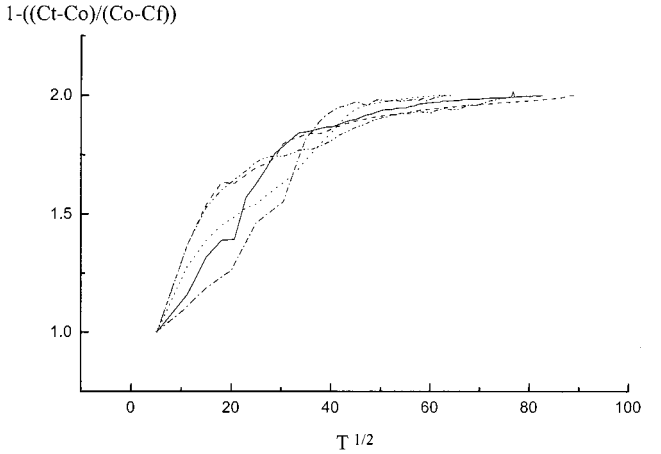

Figure 5. Normalized Electrical Conductivity for coMEX. Key: ─ coMEK E1, ─ ─ ─ coMEK E2, ··· coMEK E3, ─•─ coMEK E4, and ─••─ coMEK E5.

stage between the closely packing and coalescence stages, where the particles exist as a dense array but retain their individual identities. The onset of this stage occurred at the same time regardless of T_g; however, its duration and kinetics were T_g-dependent. A plot of the drying time at stage 1 at various temperatures for coME1−3, Figure 4a, indicates this dependence and that this stage is independent of T_g and controlled by the evaporation rate. The stage 2 drying time, Figure 4b, for the latexes at varying temperatures varies with T_g

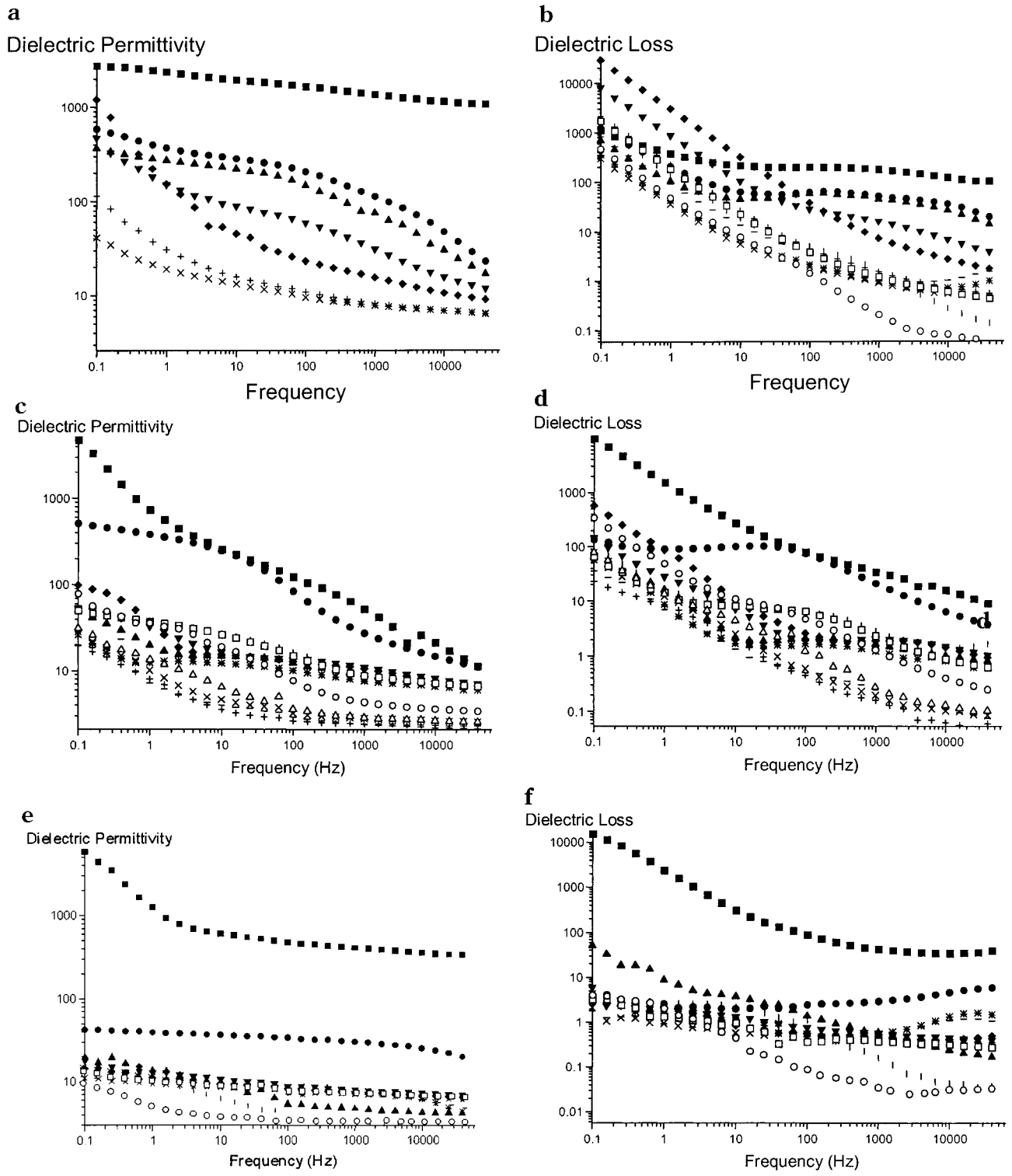

Figure 6. Change with aging time for (a) dielectric permittivity and (b) dielectric loss of coME3, (c) dielectric permittivity and (d) dielectric loss of coME4, (e) dielectric permittivity, and (f) dielectric loss of coME5. Key: ■ 0, ● 8, ▲ 9, ▼ 11, ◆ 14, + 22, **x** 23, * 30, — 35, | 36, □ 42, and ○ 49 days.

in agreement with Keddie et al.[11] These data do not indicate the way in which a drying front might be developing within the film structure and leave the question as to whether there are significant differences in the internal structure of these films to be probed by the electrical measurements.

Conductometric Analysis. Conductance measurements monitor ion movement in the aqueous phase. The data may be plotted in the form of a normalized conductance that has initially the form of pseduo-Fickian diffusion behavior;[19−21] see Figure 5. As water evaporates from the latex, the mobility of the ions in the system becomes increasingly retarded, and so, the conductance falls. The absence of the two stages in the conductance measurements is consistent with continuous changes occurring in the aqueous phase. Prior to forming a touch dry film, the aqueous phase exhibits a high conductivity because of the presence of mobile ions. As the latex solution dries, there is an initial loss of water, which causes the ion concentration and hence conductivity to increase.

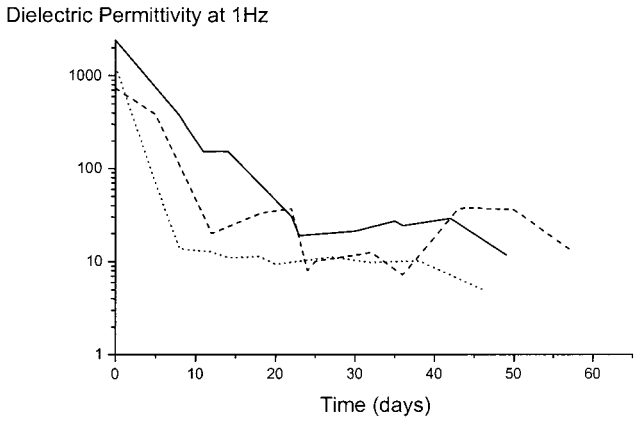

Figure 7. Dielectric permittivity (1 Hz) vs time for coME3−5. Key: — coMEK E3, — — — coMEK E4, and ··· coMEK E5.

As the solid content increases, the emulsion particles can inhibit conduction and cause the bulk conductivity to decrease. Water is lost via evaporation, and the latex particles begin to pack closely. Further evaporation will close off these channels, leaving isolated clusters containing mobile ions. Further drying reduces the mobility of the ions, and they ultimately become trapped in the polymer matrix. The conductivity can occur around the particles in the latex and therefore will not be limited by the perfect packing of the particles.

Stages Two and Three of Film Formation. *Dielectric Spectroscopy Performed Under Ambient Conditions*. The dielectric spectra were recorded for films drying at room temperature as a function of time. Dielectric spectra for three latexes, coME3−5 (Figure 6a−f), are presented to illustrate the type of behavior observed. The dielectric permittivity decreases with aging time as indicated by the change of the value at 1 Hz with time, Figure 7. Initially each film exhibits a high dielectric permittivity and loss due to the presence of residual water in interstitial sites and channels between nonuniformly packed particles. Movements of these ions will not only provide a conductivity contribution but also an interfacial polarization effect due to the inability of the film to discharge the ions at the electrodes. As the samples age, water is expelled under the forces of compaction, and consequently, the permittivity and loss values fall. Channels are created, as the particles pack will have their dielectric characteristic described by the MWS theory. The MWS contribution can be used as a guide to the heterogeneity of the sample; additionally, the conductivity contribution allows the residual water content of the films to be monitored. Analysis of the dielectric data has been discussed elsewhere.[22]

The conductivity contribution in coME3 is marked as indicated by the large values of the dielectric loss $\epsilon(\omega)''/\omega$ and is present up to 49 days of aging. This feature is less prominent in coME4 and is unseen in coME5 after 6 days. The retention of the high conductivity is an indication of the resistance to deformation of the latex particles. The coME3 latex has the highest T_g of the three latexes and hence will less readily be deformed at room temperature. As the T_g of the polymer decreases from coME4 to coME5, the particle's ability to deform increases, and hence, residual water is expelled and the conductivity contribution decreases.

Each film exhibits a decrease in permittivity with age, and Figure 7 can be related to the shift of the T_g of the

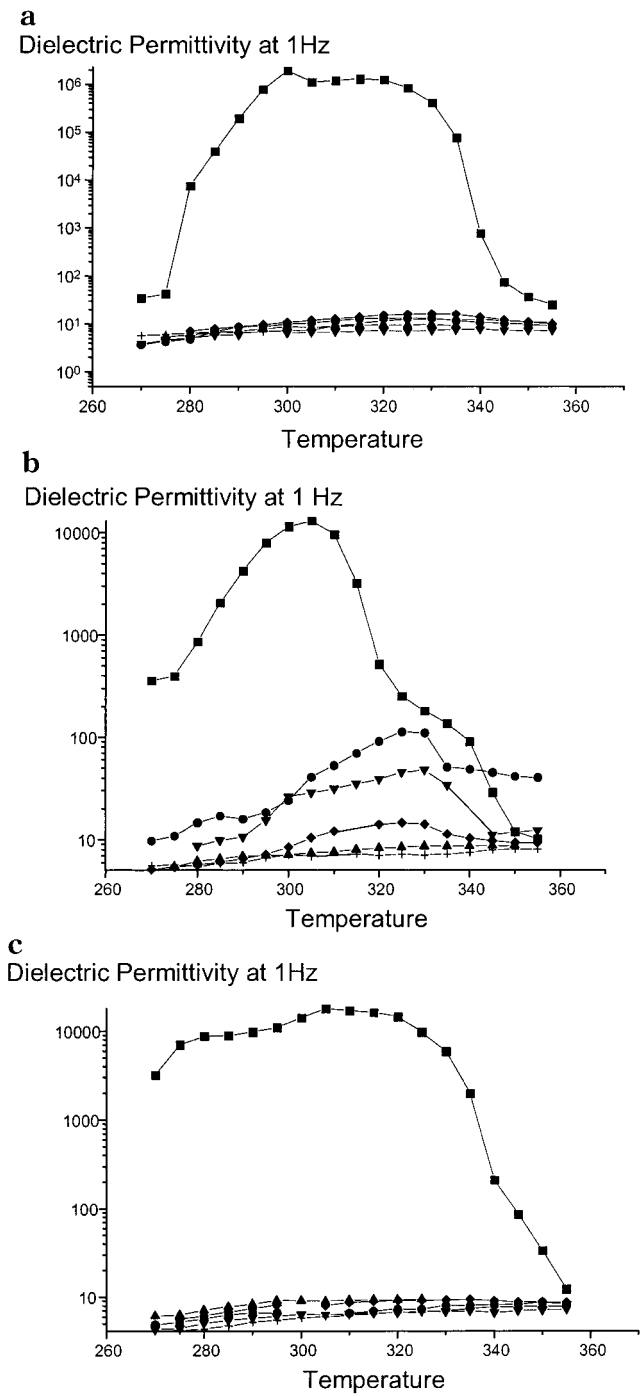

Figure 8. Change in permittivity with temperature and age for (a) CoME3, (b) coME4, and (c) coME5. Key: ■ 0, ● 4, ▲ 7, ◆ 14, ▼ 24, ◆ 14, and | 36 days.

film. MWS effects are a feature of the heterogeneity of the sample and result in large permittivity values. Reduction in permittivity is an indication of the movement toward homogeneity in the film. The permittivity of the film also depends on the amount of retained water. As the films mature and expel residual water, the permittivity should fall as the sample becomes more homogeneous. The decline in permittivity in Figure 7, as the samples age, demonstrates these two phenomena and is dependent on the T_g of the latex film. A latex film with a lower T_g will deform more readily at room temperature, and hence, water will be expelled more efficiently. These films will coalesce much quicker than a higher T_g polymer and form homogeneous films more

Table 3. Activation Energies for Relaxation Processes Seen in CoME3−5

	ΔH (kJ mol^{-1})		
sample age	coME3	coME4	CoME5
0	49.5	41.9	179.1
4	96.6	31.4	
7	76.8	11.3	
11			46.1
14	85.4	33.2	
17			15.5
24	39.9		
27			78.7
36	39.7		
42	39.7	69.4	23.7

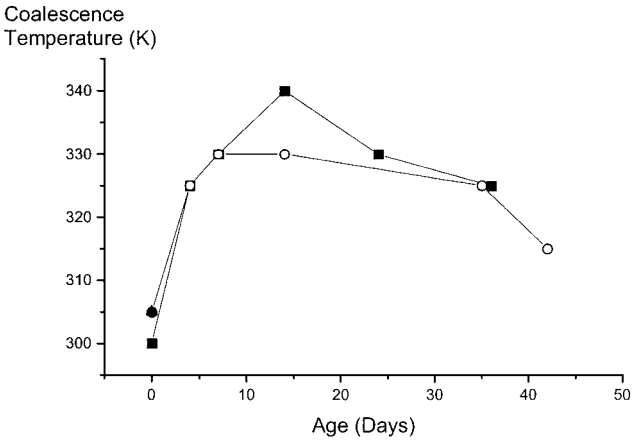

Figure 9. Change in coalescence temperature with sample age for coME3−5. Key: ■ coMEK E4, ○ coMEK E4, and △ coMEK E5.

quickly. Such a film would exhibit a lower permittivity than one of a higher T_g, Figure 7.

The MMA content of coME3 is higher than that of coME4, which has a higher MMA content than that of coME5. MMA is a more hydrophilic repeat unit than EHA; therefore, as the amount of MMA in the polymer decreases, its hydrophobicity will increase. The resultant effect will be an increased particle−water interfacial tension leading to more rapid expulsion of water from the film. The trend in dielectric permittivity shown in Figure 7 supports this theory.

Dielectric Thermal Analysis (DETA) of Thermally Aged Latex Films. Data were collected over a frequency range of 10^{-1} to 6×10^4 Hz and a temperature range of 270−355 K at an interval of 5 K, Figure 8. The temperature was equilibrated for 30 min before measurements were taken. The data obtained are complex and have been discussed in detail elsewhere.[22] All of the samples exhibit a strong conductivity contribution initially, associated with retained water that diminishes as the sample expels residual water under the forces of compaction and deformation. The conductivity contribution is retained for different time spans. In coME3, it visible in the entire aging period (36 days); in coME4, it is visible up to 14 days into maturation. For coME5, the conductivity contribution is lost before the sample is 11 days old. The retention of the conductivity contribution is an indication of the amount of water retained by the latex films, even when they are considered dry.

Relaxation processes occurring in the latex can be characterized by their activation energies, which are determined by the degree of mobility and the environment of the relaxation. As the restriction of the dipoles is increased, so the activation energy rises, Table 3. The

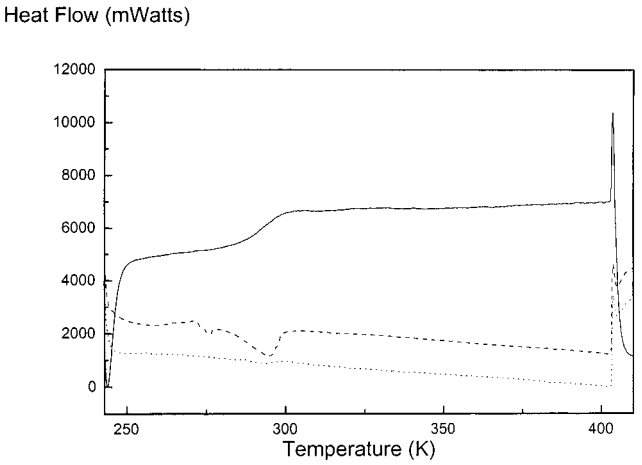

Figure 10. Typical set of DSC thermograms for calorimetric compensation analysis of latex samples. Key: — first, — — — second, and ··· third run.

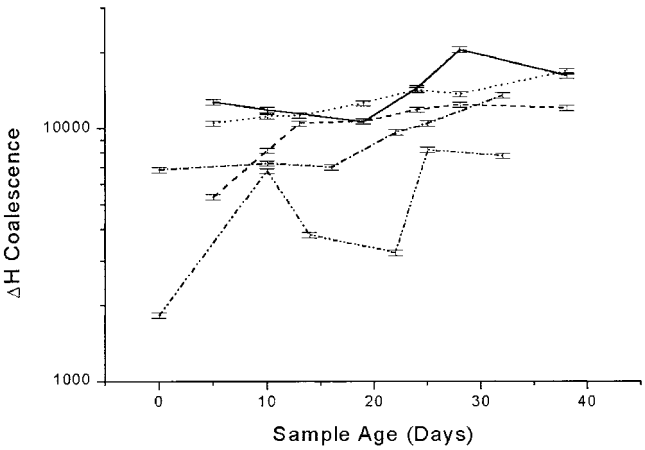

Figure 11. Enthalpy of coalescence for coMEX. Key: — coMEK E1, — — — coMEK E2, ··· coMEK E3, —•— coMEK E4, and —••— coMEK E5.

activation energies are low, indicative of side-chain motions and mobile ion migration.

A contribution from the MWS effect can be identified from a plot of the permittivity at chosen frequency against temperature, Figure 8. Large values of the permittivity are associated with the migration of ions in the channels formed by the latex. Below 273 K, the water freezes and ion mobility ceases. The studies were carried out on dry films, and the channels will have already been formed during stages 1 and 2 of drying, as studied by the conductivity experiments.

One of the main features of these profiles is the difference in magnitude of the permittivity values. coME3 exhibits a much higher permittivity value than the other two latexes, and coME4, in turn, has a higher permittivity than coME5. Because the permittivity of the bulk polymer itself must be approximately equal for the three latexes, the differences must be attributable to the amount of retained water and the degree of heterogeneity. Both of these features give rise to MWS effects and exaggerated permittivity values. It is shown that coME3 exhibits the highest permittivity value and then that of coME4, with coME5 having the lowest permittivity value, which would suggest that the degree of retained water, and therefore heterogeneity, in coME3 is higher than that for the other latexes.

A static morphology in the latex would lead to an increase in the dielectric permittivity as the dipoles

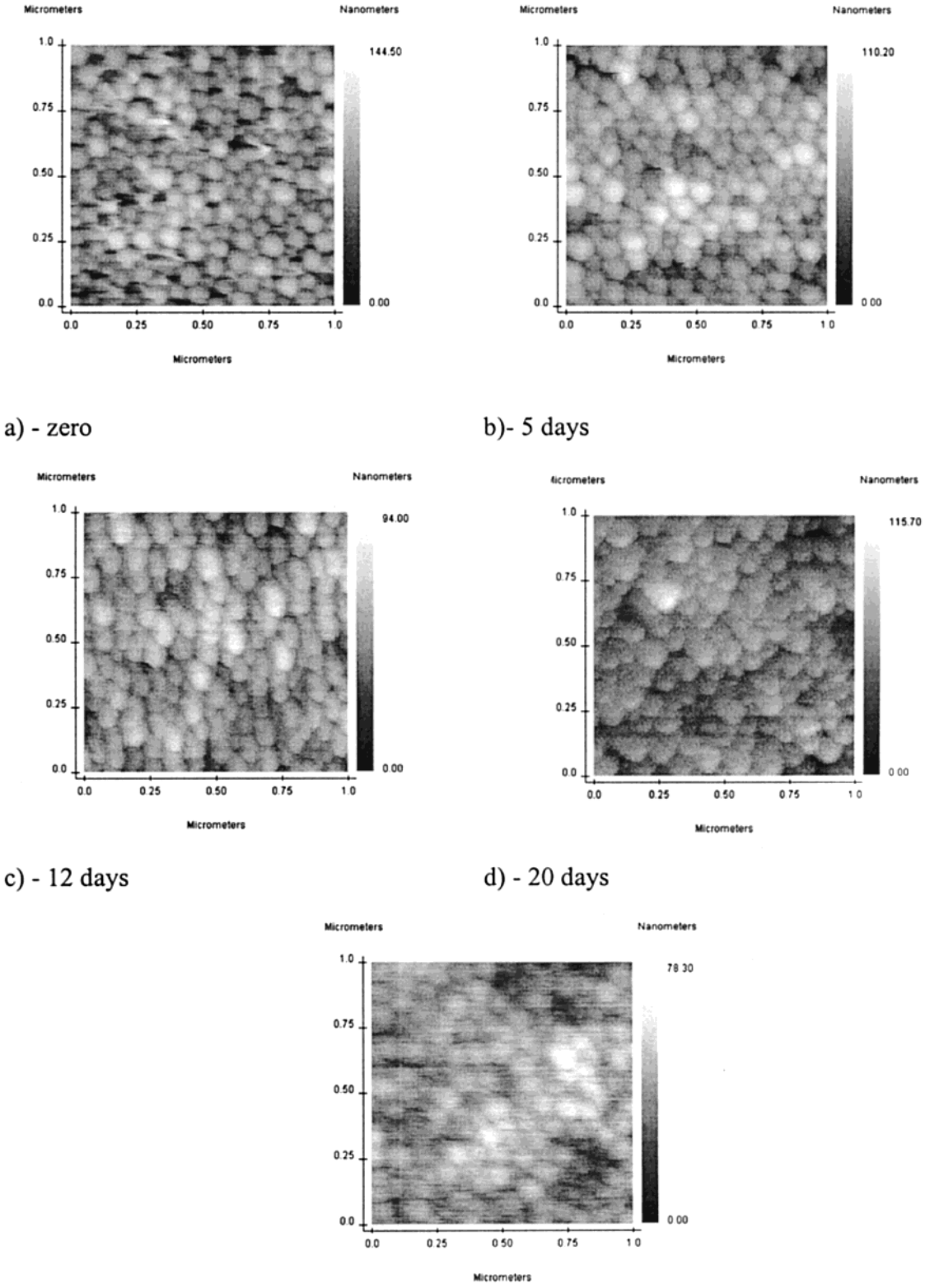

Figure 12. AFM scans of coME3 over a 33 day aging period.

attain more thermal energy with increasing temperature. A drop in the permittivity after an increase in temperature is attributed to a change in the morphology. The permittivity temperature plots for the films show a maximum permittivity value, and the subsequent decrease is indicative of a change in morphology beyond this temperature. Coalescence is the main cause of a change in the morphology and can directly be identified from the dielectric temperature profile, Figure 8. A plot of the variation in coalescence temperature as the samples age is shown in Figure 9. The lower T_g films exhibit lower coalescence temperatures, and their values increase with maturation of the film as a of result the loss of water from the latex system. Water acts as an internal plasticizer, and as it is expelled during compaction, the T_g of the outer hydrophilic membranes will

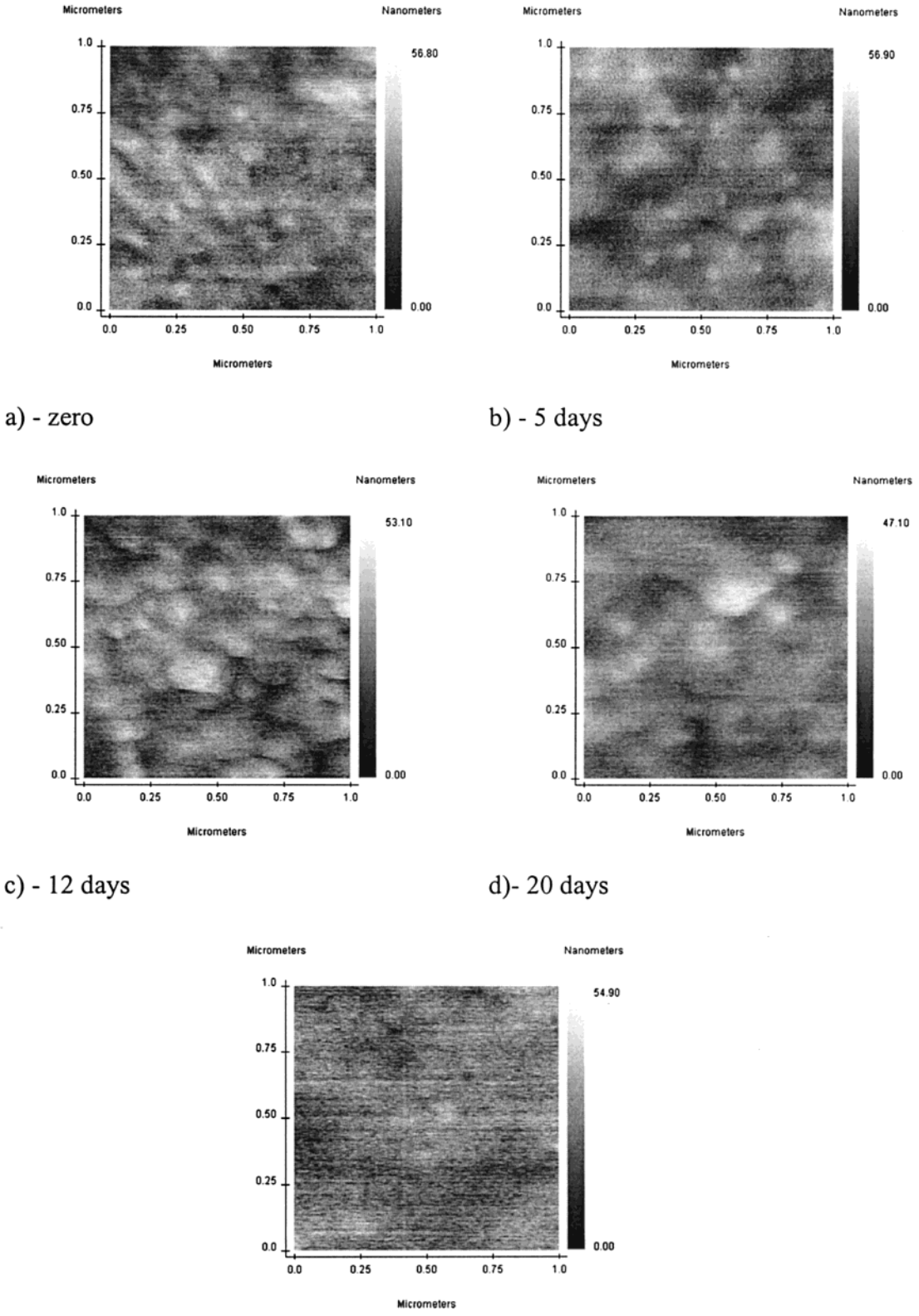

Figure 13. AFM scans of coME5 over a 33 day aging period.

increase; hence, more energy will be required to accelerate coalescence in the film. After a period of aging, the coalescence temperature decreases, indicating that a lower energy input to the system is required to force coalescence. Natural compaction and deformation of the latex particles during aging will increase close packing and hence will reduce the amount of work required to facilitate full coalescence. In addition, lower T_g polymers are shown to deform faster at room temperature; therefore, the degree of close packing will be greater. This phenomenon is especially evident in coME5, which exhibits only one coalescence temperature, suggesting that its passage to homogeneity is a rapid one.

*Differential Scanning Calorimetry: Calorimetric Compensation Method***.** A typical example of the data, Figure 10, was obtained with 20−30 mg and was measured

over a temperature range of 243−403 K at a heating rate of 10 K min^{-1} and using a sensitivity range of 5 mcal. The first run exhibits a clear thermal step indicative of the T_g. The second run contains an exothermic peak associated with the coalescence process. The energy of coalescence will be influenced by a number of factors: (i) the loss of residual moisture from the system, (ii) the rearrangement and redistribution of the stabilized layer of the system, and (iii) the energy associated with the motion of polymer chains across the latex interface to form a coalesced film.

The film-forming properties will determine the enthalpy of disappearance of the specific surface. It is, therefore, reasonable to assume that this enthalpy of coalescence will vary depending on T_g and the MFFT through their influence on compaction and deformation. The DSC was standardized using indium, whose enthalpy of fusion is 28 451.1 J/kg.[15] The mean enthalpy of fusion from 10 measurements was 27 982.1 J/kg, giving an associated error of 1.6%. The standard deviation of the data obtained, 80.7 J/kg, corresponds to a reproducibility of 0.29%.The method is based on the reversibility of the system's heat capacity, heat conductivity, and second-order glass transition. The data reported hereafter were recorded from the second day of drying until the end of the aging period. The thermograms observed were similar to those shown in Figure 10. Each thermogram displayed an exothermic peak linked to the disappearance of the specific surface of the latex particles (coalescence). Each peak was integrated to determine the relative enthalpy of coalescence for each sample. The exothermic peak represents the disappearance of the interface (coalescence) and was measured during the aging process. A relative enthalpy of coalescence was determined for each sample, and this quantity was followed throughout the maturation process; see Figure 11. The errors bars displayed on the graphs represent the uncertainty of the DSC. The data show a decrease in the enthalpy of coalescence as the T_g of the sample decreases from coME1 to coME5. The enthalpies of coalescence for coME1−4 are very similar. The ΔH increases as the sample ages. Surfactants, by their nature, are surface-active and are often desorbed to the film−air and film−substrate interfaces during maturation. However, SDS can be retained at the particle surface. Retention of SDS in the interparticle zone will increase the T_g of the interface around the particles by dipolar interactions between the polar headgroups of SDS and the polymer chain. The consequence is an increase in the amount of energy required to promote coalescence.

As two latex particles are brought into close contact, their absorbed outer layers of surfactant begin to interpenetrate and the polar headgroups are brought close to the particle surface. The surface will tend to be enriched with the more hydrophilic component, methyl methacrylate. Therefore, the ionic headgroups are brought into contact with the acrylate groupings at the particle surface. This leads to the formation of dipolar interactions between the two groupings. An increase in the T_g of the polymer results from a restriction in the chain mobility, both in the backbone and in the rotational motion of side groups. As the sample ages, it will increasingly deform and the latex particles will become more closely packed. A greater degree of close packing will ensure that more ionic headgroups will be brought into close contact with the particle surface.

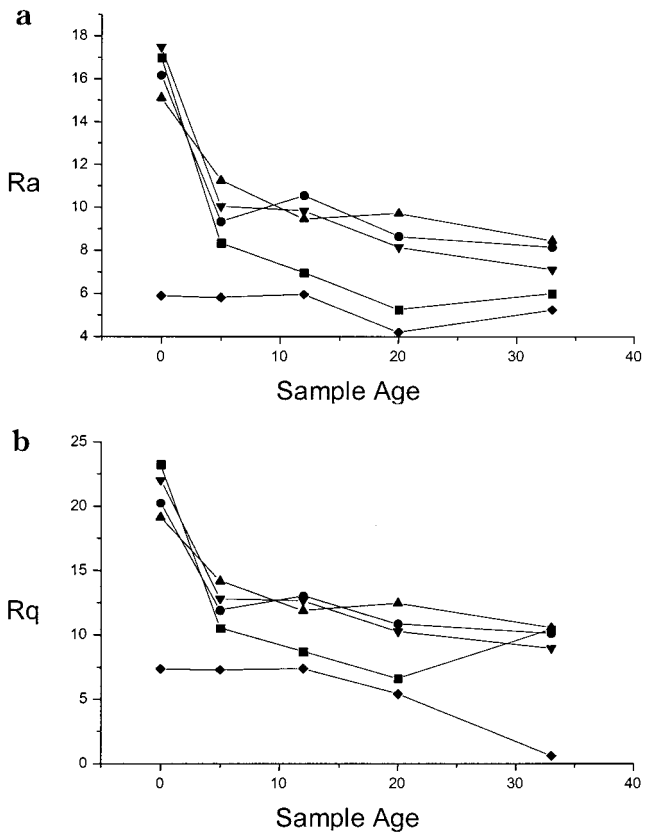

Figure 14. (a) Height variance and (b) root-mean-square statistical analyses for coMEX images. Key: ■ coMEK E1, + coMEK E2, ▲ coMEK E3, ▼ coMEK E4, and ◆ coMEK E5.

Atomic Force Microscopy. AFM provides a method of visually following the changes occurring in a sample as it matures. AFM allows statistical analysis to be performed on the scans of the sample surface and provides information on surface roughness as aging occurs. An illustration of the traces obtained for two systems are presented in Figures 12 and 13 for coME3 and coME5. It can be assumed that a decrease in surface roughness will be indicative of an increase in the degree of coalescence. Initially, the structure seen is that of a closely packed structure, although it is very faint in coME5, Figure 14b. The AFM scans show that the closely packed pattern is retained in coME3 over the aging period studied. The images depicted in Figure 14b, show a degree of surface roughness, and however, it can be concluded that coalescence has occurred in this sample. The AFM scans are influenced by the presence of water that can have adverse effects on the clarity of the image. Statistical analysis was performed on the entire image and is quoted in terms of the three statistical quantities: R_q (the root-mean-square of the surface), R_a (the height variance of the surface), and R_{p-p} (the height difference between the highest and lowest points on the surface).

The retention of the spherical pattern of latex beads in samples coME3 confirms the results obtained by dielectric spectroscopy and DSC, which indicated that coalescence had not occurred in these samples at this degree of aging. Statistical analysis was performed on the AFM images, and the results are shown in Figure 14. The statistical analysis indicates that as the coalescence occurs so the roughness of the surface decreases. The statistics indicate that coalescence in coME5 is rapid, which is confirmed by the scans.

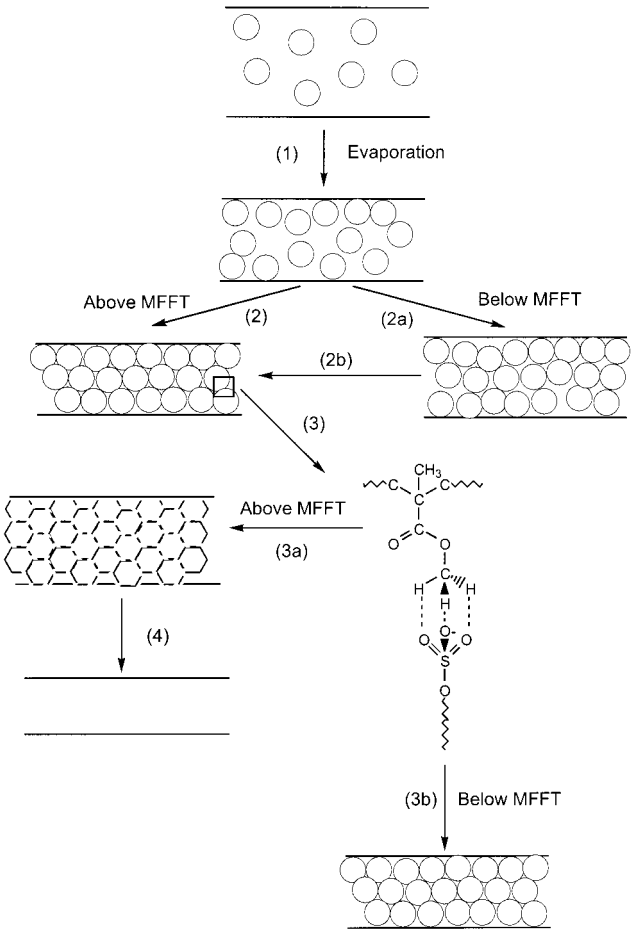

Figure 15. Model of the influence of viscoelastic effects of film formation.

Conclusions

The five latexes were studied in order to probe the effects of the glass-transition temperature on the film-formation processes, Figure 15. The data leads to the proposal of a model from film formation in these systems; the model is complex and involves several stages. These can be explained as follows. (1) Evaporation of water from the latex results in a higher solids fraction. (2) If the latex is dried at a temperature that is higher than its MFFT, then the evaporation kinetics are constant until a dense packing of spheres is obtained. (2a) However, if the latex is dried at a temperature that is lower than its MFFT, then a two-stage drying model results. The additional stage occurs at approximately 0.7 volume fraction and is associated with the resistance to deformation of the polymer particles at this temperature. (2b) Evaporation continues until the latex exists as a dense array of closely packed spheres. The duration of stages 2a,b are dependent on the viscoelastic nature of the polymer itself. (3) The formation of a dense array of latex spheres is facilitated by the expulsion of residual water and compaction of the latex to ensure a closely packed environment. This action also brings the absorbed outer layers of the particles into close contact and causes them to interpenetrate; thus, the sulfate headgroup of the surfactant molecule comes into close contact with the acrylate groupings on the polymer chain. The net result is the formation of hydrogen bonds between the sulfate and acrylate groups. As the latex ages, these groups will be brought into closer contact and the formation of hydrogen bonds will be more favorable. These bonds serve to restrict the motion of the polymer chain and hence increase the T_g of the outer particle membranes. (3a) The latex has two factors influencing its coalescence. First, the presence of surfactant-related hydrogen bonds that increase the T_g of the particle membrane and effectively inhibit coalescence. And second, the particles' own resistance to deformation. When the film exists at a temperature that is higher than its MFFT, its resistance to deformation is slight and can outweigh the effects imposed by the surfactants. In such a case, the latex particles can deform to fill available space. (3b) When a latex exists at a temperature lower than its MFFT, its resistance to deformation is strong; coupled with the inhibitive effects of surfactant-related hydrogen bonds, it becomes very difficult for these latexes to deform to fill the available space. (4) Once the latex has deformed to fill available space, the particle membranes can start to break up and allow interparticle diffusion to occur. The result is a homogeneous film with no boundaries.

A number of theories have been developed that describe the way in which the drying front develops and its influence on the film-forming properties.[5−8] The conclusions drawn from this paper are in general consistent with the currently accepted views of the progression of the drying front within the film and the extent to which organized structure is developed within the film. This study does identify that there are various stages that can be identified and allows for consideration as to whether further refinement is appropriate.

Acknowledgment. L.C. thanks the EPSRC and ICI (Paints) for the support of a CASE studentship for the period of this research. We wish to thank Drs. D. Taylor and D. Elliott for their help and guidance during the course of this study.

References and Notes

(1) Eckersley, S. T.; Rudin, A. *Film Formation in Waterbourne Coatings*; Provder, T., Winnik, M. A., Urban, M. W., Ed.; ACS Symposium Series 648; American Chemical Society: Washington, DC, 1996; p 2.
(2) Niu, B. J.; Martin, L. R.; Tebelius, L. K.; Urban, M. W. *Film Formation in Waterbourne Coatings*; Provder, T., Winnik, M. A., Urban, M. W., Ed.; ACS Symposium Series 648; American Chemical Society: Washington, DC, 1996; p 301.
(3) Keddie, J. L.; Meredith, P.; Jones, R. A. L.; Donald, A. M. *Film Formation in Waterbourne Coatings*; Provder, T., Winnik, M. A., Urban, M. W., Ed.; ACS Symposium Series 648; American Chemical Society: Washington, DC, 1996; p 332
(4) Ming-Da, Eu; Ullman, R. *Film Formation in Waterbourne Coatings*; Provder, T., Winnik, M. A., Urban, M. W., Ed.; ACS Symposium Series 648; American Chemical Society: Washington, DC, 1996; p 79
(5) Winnik, M. A. *Film Formation in Waterbourne Coatings*; Provder, T., Winnik, M. A., Urban, M. W., Ed.; ACS Symposium Series 648; American Chemical Society: Washington, DC, 1996; p 51.
(6) Routgh, A. F.; Russel, W. B. *AICHE J.* **1998**, *44* (9), 2088.
(7) Feng, J. R.; Winnik, M. A. *Macromolecules* **1997,** *30* (15), 4324.
(8) Wang, Y. C.; Winnik, M. A. *J. Phys Chem.* **1993**, *97* (11), 2507.
(9) Winnik, M. A.; Winnik, F. M. Advances in Chemistry Series 236; American Chemical Society: Washington, DC, 1993; p 485.
(10) Sperry, P. R.; Snyder, B. S.; O'Dowd, M. L.; Lesko, P. M. *Langmuir* **1994**, *10*, 2619.
(11) Keddie, J. L.; Meredith, P.; Jones, R. A. L.; Donald, A. M. *Macromolecules* **1995**, *28*, 2673−2682.
(12) Rodriguez, F. *Principles of Polymer Systems*, 2nd Ed.; Wiley: New York, 1992.

(13) O'Callaghan, K. J.; Pain, A. J.; Rudin, A. *J. Polym. Sci. Part A, Polym. Chem. Ed.* **1995**, 33 (11), 1849−1857.
(14) Mahr, T. G. *J. Phys. Chem.* **1970**, *74*, 2160.
(15) Perkin-Elmer *DSC Manual*, 1994.
(16) Hayward, D.; Gawayne, M.; Mahboubian-Jones, B.; Pethrick, R. A. *J. Phys. E: Sci. Instrum.* **1984**, *17*, 683.
(17) *AFM Reference Manual*; Burleigh, 1995.
(18) Harkins, W. D. *J. Chem. Phys.* **1945**, *13*, 381.
(19) Harkins, W. D. *J. Chem. Phys.* **1946**, *14*, 47.
(20) Harkins, W. D. *J. Am. Chem. Soc.* **1947**, *69*, 1428.
(21) Harkins, W. D. *J. Polym. Sci.* **1950**, *5*, 217.
(22) Cannon, L.; Hayward, D.; Pethrick, R. A., submitted for publication.
(23) Cannon, L. Ph.D. Thesis, University of Strathclyde, Glasgow, Scotland, 1998.

MA990273I